Rotational Isomerism and Atropisomerism in Acetal Derivatives of 1,2,3,4-Tetrafluorotriptycene-9-carbaldehyde

Gaku YAMAMOTO
Department of Chemistry, Faculty of Science, The University of Tokyo, Bunkyo-ku, Tokyo 113
(Received March 23, 1992)

In the ethylene acetal (**2**) of 1,2,3,4-tetrafluorotriptycene-9-carbaldehyde, equal amounts of the *ap* and $\pm sc$ rotamers exist in $CDCl_3$ at equilibrium, while the equilibrium is strongly shifted to $\pm sc$ in the corresponding dimethyl and trimethylene acetals. Molecular mechanics calculations reveal the origin of this anomaly to reside in the conformation of the acetal moiety. Dynamic NMR studies show that the $ap \rightarrow \pm sc$ barriers are too low for atropisomerism to be realized in these compounds ($\Delta G^{\ddagger}$ ca. 21—22 kcal mol^{-1} (1 cal_{th}=4.184 J)). However, taking advantage of the unusual equilibrium behavior, the two rotamers of **2** are separately isolated as crystals by selective crystallization of one rotamer from a solution of the equilibrated rotamer mixture.

Equilibrium among conformers of a molecule is subject to various factors of steric as well as electronic origin. Observation of apparently abnormal behavior of conformational equilibria has often lead to a new idea of intramolecular interaction or revealed unique conformational states of the molecules. Studies of rotamer equilibria about the bridgehead-to-substituent bond in 9-substituted triptycene derivatives have afforded abundant information on various types of intramolecular interaction between the substituent at the bridgehead and the one at the *peri* position of the triptycene skeleton, taking advantage of high energy barriers to rotation about the bond.[1]

The high rotational barrier has allowed some 9-substituted triptycene derivatives to show atropisomerism, i.e., stereoisomerism due to restricted rotation about a single bond in which stable rotational isomers can actually be isolated.[2,3] Examples of atropisomerism about an sp^3–sp^3 carbon bond are rather rare.[4–11] Among triptycene compounds only 9-*t*-alkyltriptycene derivatives[6–9] and triply or doubly *peri*-substituted 9-arylmethyltriptycenes have given rise to atropisomers.[10,11] Atropisomerism in 9-*s*-alkyltriptycenes has not yet been reported, although the rotational barriers reach 24 kcal mol^{-1} in some cases.[12–15]

Atropisomerism has so far been realized by isolating a pure rotamer in solution as the first step, then removing the solvent to get the pure rotamer in a crystalline state. Thus the rotamer should have a rotational barrier high enough to retain its identity in solution for a sufficiently long period. Free energy of activation of 24 kcal mol^{-1} has been claimed as the threshold value, which corresponds to a rate constant of 1.6×10^{-5} s^{-1} at 25 °C and a half-life of the rotamers of ca. 6 h when two rotamers are equally populated at equilibrium.

With an aim to obtain 1,2,3,4-tetrafluorotriptycene-9-carbaldehyde (**1**), we synthesized the corresponding ethylene acetal **2** because the formyl group should be properly protected in the benzyne reaction. We found an intuitively unusual behavior of the rotamer equilibrium and decided to investigate these points in some detail. For comparison, several other acetals of **1**, i.e., trimethylene acetal **3** and dimethyl acetal **4** were synthesized. In this article, experimental data on the rotamer equilibria and rotational barriers of these compounds are reported and discussed together with the results of molecular mechanics calculations.[16]

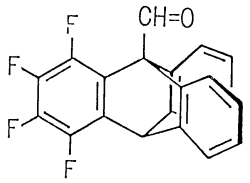

1

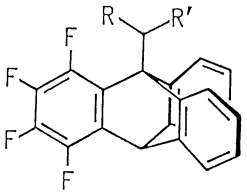

2: R,R'=OCH_2CH_2O
3: R,R'=$OCH_2CH_2CH_2O$
4: R=R'=OCH_3
8: R=R'=CH_3
9: R=OCH_3, R'=CH_3

Two rotational isomers of **2** were separately isolated as crystals by selective crystallization of one rotamer from a solution of the equilibrium mixture of the rotamers taking advantage of the presence of two rotamers in equal amounts at equilibrium despite of the fact that the rotational barrier is lower than the threshold value mentioned above. The details are also described in this paper.[16]

Results and Discussion

Syntheses. Anthracene-9-carbaldehyde was converted to acetals **5**—**7**, which were then reacted with tetrafluorobenzyne generated in situ by thermal decomposition of pentafluorophenyllithium to give 1,2,3,4-tetrafluorotriptycenes **2**—**4**. A considerable amount of the 1,4-adduct, 6-substituted 1,2,3,4-tetrafluoro-5,12-dihydro-5,12-ethenonaphthacene, was formed as a by-product. The reaction mixture containing the desired triptycene, the 1,4-adduct, and the unreacted starting anthracene was treated with dilute hydrochloric acid at ambient temperature before subjecting to column

chromatography. The acetal moieties of the 1,4-adduct and the anthracene were rapidly hydrolyzed while the acetal moiety of the triptycene resisted hydrolysis probably because of the steric hindrance. Thus the chromatographic purification of the triptycene was easily performed.

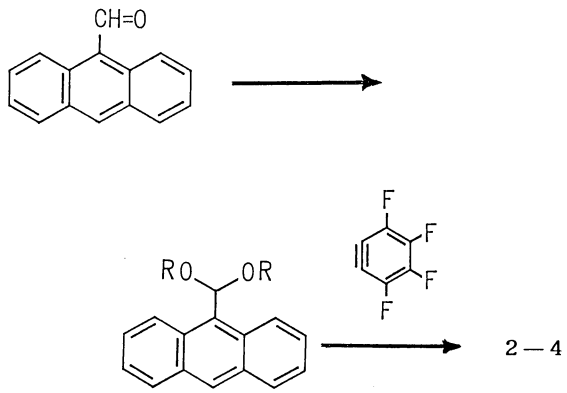

5: R,R=CH_2CH_2
6: R,R=$CH_2CH_2CH_2$
7: R=CH_3

Rotamer Equilibria in Solution. In each of the triptycene acetals, two kinds of rotamers, *ap* and ±*sc*, were found to exist in solution at equilibrium (see the Newman projections in Scheme 1, where R=R′). As discussed in detail in a later section, the internal rotation of the bridgehead-to-substituent bond in these compounds was somewhat fast on the laboratory time scale although it was very slow on the NMR time scale. When a crystalline sample of the triptycene acetals was dissolved in $CDCl_3$ and immediately subjected to the NMR measurement, the rotamer composition was often deviated from the equilibrium value, although the equilibrium was attained within several hours at ambient temperature.

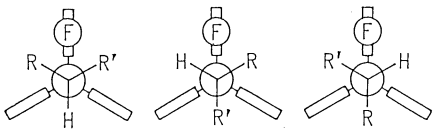

Scheme 1.

Rotamer assignments were easily made by ^1H NMR because the *ap* rotamer had plane symmetry (C_s) on the NMR time scale and the ±*sc* rotamer had no symmetry: e.g. the CH_2CH_2 signal in **2** showed a typical AA′BB′ pattern in the *ap* rotamer and an ABCD pattern in the ±*sc* rotamer.

Equilibrium populations of rotamers of **2**—**4** in $CDCl_3$ at 26 °C are given in Table 1 together with the previously reported data for the related compounds **8**[12b] and **9**.[15a]

Comparison of the data for **4**, **8**, and **9** reveals an important feature. In 1,2,3,4-tetrafluoro-9-isopropyltriptycene (**8**), the population of the *ap* rotamer was 10%, which was reasonably ascribed to steric effects.[12b] Successive replacements of the methyl groups in **8** by a methoxyl group (**8**→**9**→**4**) lowered the population of *ap*, while the reverse should be expected if only the steric effect was considered, because a methoxyl group was thought to be less bulky than a methyl group. The observed trend therefore suggested that the electrostatic effect, i.e. Coulombic repulsion between 1-F and the methoxyl oxygen(s), overweighed the steric effect. Compound **3** behaved similarly as **4**. If these findings were taken into account, the very large population as much as 50% of *ap*-**2** (Table 1) seemed quite unusual.

The rotamer populations of **2**—**4** were studied in various solvents and the results are shown in Table 2. Here again **2** behaves differently from **3** and **4**. As the polarity of the solvent increases, the population of the *ap* rotamer increases in **3** and **4** but decreases in **2**, although the magnitude of the change is small in any compound.

In order to clarify these astonishing difference in rotamer equilibria between **2** and **3** or **4**, we performed

Table 1. Rotamer Equilibria in $CDCl_3$ at 26 °C[a]

Compd	Population/%			K[(**B1**+**B2**)/**A**]
	A	**B1**	**B2**	
2	50	50		1.00±0.02
3	8	92		11.6 ±0.5
4	3	97		32 ±2
8[b]	10	90		9.0 ±0.2
9[c]	6	39	55	16 ±1

a) See Scheme 1 for **A**, **B1**, and **B2**. b) Ref. 12b. c) Ref. 15a.

Table 2. Solvent Effects on Rotamer Equilibria[a]

Solvent	**2**		**3**		**4**	
	K(±*sc*/*ap*)	%*ap*	K(±*sc*/*ap*)	%*ap*	K(±*sc*/*ap*)	%*ap*
C_6D_{12}	0.65±0.02	61	9.7±0.5	9.3	36 ±2	2.7
C_6D_6	0.86±0.02	54	9.8±0.5	9.3	25 ±2	3.8
$CDCl_3$	1.00±0.02	50	11.0±0.5	8.3	32 ±2	3.0
CD_3CN	1.38±0.02	42	8.6±0.5	10.4	15.5±1.0	6.1

a) Measured at 26 °C by ^1H NMR (500 MHz).

molecular mechanics calculations and analyzed the energy deta (Table 3). Calculations were carried out using the BIGSTRN3 program[17] with a modified MM2 force field. The components of the relative steric energy (E_s) were divided into two terms, i.e., the electrostatic term and the rest, the latter being referred to as "steric", as shown in Table 3.

The calculated E_s values are somewhat deviated from the $\Delta H°$ values calculated from the observed rotamer ratio by assuming that only the degeneracy of $\pm sc$ form contributes to the entropy difference $\Delta S°$, i.e., $\Delta S° = R \ln 2$. However the trend that the *ap* rotamer is less and less stabilized on going from **2** to **3** to **4**, is well reproduced.

The component analysis reveals that the extent of contribution of the electrostatic term on the ground state energy is significantly different among the compounds while the "steric" term contributes similarly in any compound. In **2** the electrostatic term is rather unimportant in determining the relative stability of the rotamers and slightly favors the *ap* rotamer while in **4** this term greatly destabilizes the *ap* rotamer. Compound **3** shows an intermediate behavior between **2** and **4**.

These features are also revealed by inspection of the molecular geometries of the rotamers. The optimized geometries of the rotamers of **2** and **4** are shown in Fig. 1. The most significant difference between the geometries of **2** and **4** is in the conformation of the acetal moiety. In either rotamer of compound **2**, the five-membered ring adopts an envelope conformation in which the O–C–C–O moiety is planar and C_α is away from this plane, and the C_9–C_α bond is pseudoequatorial. In compound **4**, the C_9–C_α–O–C moieties deviate from the strictly staggered conformation because the two methyl groups repel each other. Thus the methyl carbons in **4** are more distant from each other than the methylene carbons in **2**. According to these features, the dipoles of the two C–O–C linkages constitute a sharper vector angle in **4** than in **2**, as revealed by the arrows given in Fig. 1. The electrostatic interaction between the tetrafluorobenzeno moiety and the C–O–C moieties is expected to strongly destabilize the *ap* rotamer of **4** relative to *ap*-**2**, while the same factor destabilizes $\pm sc$-**2** to some extent relative to $\pm sc$-**4**, resulting in large instability of the *ap* rotamer in **4**

Table 3. Results of the Molecular Mechanics Calculations[a]

Compd	**2**		**3**		**4**	
	$\pm sc$	*ap*	$\pm sc$	*ap*	$\pm sc$	*ap*
$\Delta H°$[b]	0	−0.41	0	1.05	0	1.79
E_s	0	0.56	0	1.71	0	2.22
"Steric"	0	0.79	0	0.73	0	0.69
Electrostatic	0	−0.23	0	0.98	0	1.53
Dipole moment[c]	3.63	4.51	3.55	5.21	3.54	5.72

a) Energies are calculated by BIGSTRN3 and are given in kcal mol^{-1} relative to $\pm sc$. b) Calculated from the observed rotamer ratio assuming $\Delta S° = R \ln 2$. c) Calculated by MM2 and given in D.

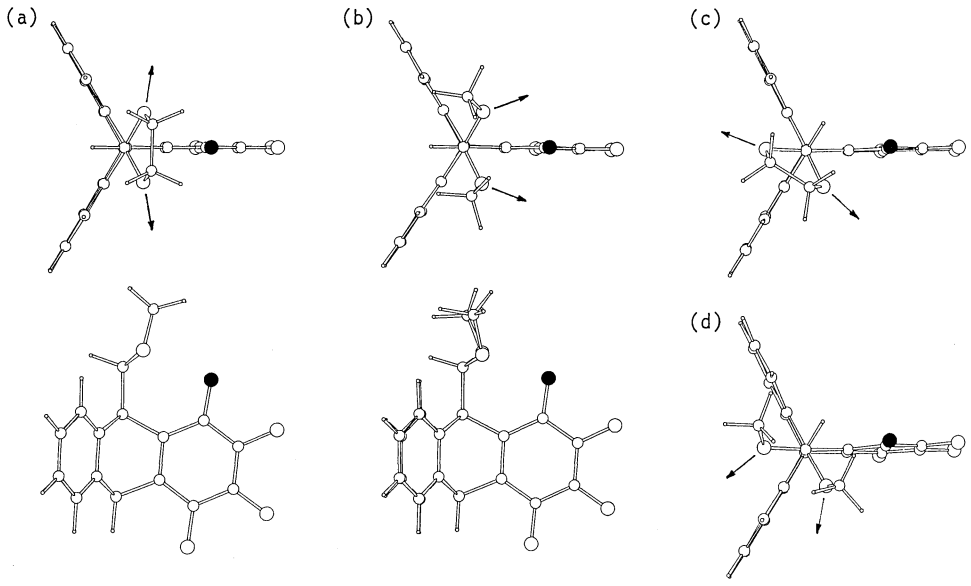

Fig. 1. The BIGSTRN3 optimized geometries of (a) *ap*-**2**, (b) *ap*-**4**, (c) $+sc$-**2**, and (d) $+sc$-**4**. Arrows show the direction of the C–O–C dipoles. Black circles indicate the 1-F atoms.

and comparable stability of two rotamers in **2**, as revealed by the energy consideration mentioned above.

These structural features are reflected in the ^{1}H NMR chemical shifts. In the ±*sc* rotamer, the *peri* protons, 8-H and 13-H, are nonequivalent. The chemical shifts of 13-H flanked by two oxygens are δ=7.68, 8.37, and 8.19 for **2**, **3**, and **4**, respectively, in $CDCl_3$ at 26°C, while those of 8-H are δ=7.73, 7.47, and 7.30, respectively. Namely, the 13-proton in **3** and **4** resonates at a lower field by 0.8—0.9 ppm than the 8-proton because of the anisotropy and field effects of the ether linkages, while the 13-proton in **2** appears 0.05 ppm *higher* than the 8-proton. These spectral features are consistent with the geometries shown in Fig. 1.

No clear-cut explanation for the solvent effect on the rotamer equilibria (Table 2) can so far be given. According to the MM2 calculation the ±*sc* rotamers of **2**—**4** have almost the same dipole moments, while the *ap* rotamers have larger moments than the respective ±*sc* rotamers and the values significantly increase on going from **2** to **3** to **4** (Table 3). This might suggest that the population of the *ap* rotamer would increase as the solvent becomes more polar in any compound, which is contrary to the experimental results. This may partly be ascribed to the inadequacy of the force field parameters.

Atropisomerism in 2. As described in the previous section, interconversion among rotamers in the present compounds takes place rather rapidly at ambient temperature and realization of atropisomerism in a traditional sense is impossible. If one of the rotamers selectively crystallizes out from a solution of an equilibrating mixture of rotamers under some conditions, and the other rotamer crystallizes under the other conditions, then two of the rotamers will be isolated separately as crystals. These situations seem likely to occur especially when two rotamers are present in comparable amounts as in **2**.

When the crystals of **2** with an unknown rotamer ratio were dissolved in CH_2Cl_2 (ca. 5 ml per 100 mg of **2**) and about the same volume of hexane was added, rapid crystallization took place probably because of supersaturation. The rotamer ratio ±*sc*/*ap* of the crystalline samples of **2** obtained in this way was found to change from time to time in the range of 1 to 3 as revealed by ^{1}H NMR measured immediately after dissolution of the samples in $CDCl_3$. Predominance of the ±*sc*-rotamer may be due to the slightly lower solubility and better crystallizability of this rotamer.

When an appropriate amount of hexane was added to a solution of **2** in CH_2Cl_2 so that the resulting solution was not supersaturated, and the solution was left standing at ambient temperature so that slow evaporation of the solvent occurred, pure crystalline ±*sc*-**2** was obtained, which showed a melting point of 228—230°C by conventional mp measurement. Dissolution of the sample in $CDCl_3$ below 0°C and measurement of NMR at ca. 0°C gave spectra of pure ±*sc*-**2**, the data being given in the Experimental Section.

Selective crystalliation of *ap*-**2** was rather difficult and many trial-and-error experiments were made. The fact that the population of the *ap* rotamer increased with the decrease in the solvent polarity (Table 2) suggested that saturated hydrocarbons would be suitable for the recrystallization solvent. As **2** hardly dissolved in hexane, higher boiling 2,2,4-trimethylpentane (so-called "isooctane") was chosen. Compound **2** was dissolved in boiling isooctane and the solution was kept at 40—45°C so that the solvent slowly evaporated. The *ap* rotamer of **2** was selectively crystallized as granules, mp 226—230°C, although the ±*sc* rotamer occasionally crystallized together. NMR spectral data of the pure *ap* rotamer were similarly obtained at low temperatures as mentioned above for the ±*sc* rotamer.

Once crystals of the pure rotamers were obtained, selective crystallization of either of the rotamers became easy by seeding small pieces of the crystals.

Thus two rotamers (atropisomers) were separately isolated as crystals and this constitutes the first example of atropisomerism in 9-*s*-alkyltriptycene derivatives.

The fact that the rotameric crystals of **2** show almost the same melting point (mp) may suggest that in either or both rotamers isomerization takes place in solid state during the course of heating up to the mp and that they are in the same state when they melt. We have found such a case in the atropisomeric forms of 8-halo-1,4-dimethyl-9-(2-methylbenzyl)triptycenes where the halogen is chlorine or bromine.[11b,c] A detailed study on the solid-state behavior of the atropisomers of **2** is in progress and will be reported elsewhere.

Careful recrystallization of **3** or **4** from common solvents gave the pure ±*sc* rotamer in a crystalline form because of the large population of the rotamer in solution. Attempts to purely isolate the *ap* rotamer of these compounds has not been made.

Rotational Barriers. As qualitatively revealed in the previous sections, the internal rotation of the bridgehead-to-substituent bond in **2**—**4** is slow on the NMR time scale but fast on the laboratory time scale at ambient temperature with the energy barriers of around 20 kcal mol^{-1}. A quantitative study on the rotational barriers in these compounds seemed worthwhile because these compounds could serve as a model system with appropriate barrier heights where several independent approaches could be made, i.e. classical kinetics, ^{1}H total lineshape analysis, and ^{1}H saturation transfer experiments.

The pure rotamers of **2** isolated as crystals isomerize rapidly in solution at ambient temperature to afford an equilibrium mixture of rotamers. Detailed kinetic studies of isomerization were made starting from pure ±*sc*-**2** in $CDCl_3$ at 26 and 34°C. By following the change in the relative intensities of the methyl proton signals at appropriate intervals and analyzing the data as a first-order reversible process by use of the least squares

Table 4. Kinetic Data for Internal Rotation

Compd	Process	Method[a]	Temp °C	K $\pm sc/ap$	k s^{-1}	$\Delta G^{\ddagger}$[b] kcal mol^{-1}	$\Delta H^{\ddagger}$ kcal mol^{-1}	$\Delta S^{\ddagger}$ cal mol^{-1} K^{-1}	Solvent
2	$+sc \rightleftharpoons -sc$	TLA	86		92	17.9[c]	18.0±0.6	0.3±1.7	C_6D_5Br
			78		52				
			73		34				
			67		21.5				
			59		11.0				
	$\pm sc \longrightarrow ap$	TLA	135	1.12	12.5	22.1			C_6D_5Br
			125	1.10	6.4	22.1			
		CK	34	1.00	1.23×10^{-3}	22.1			$CDCl_3$
			26	1.00	4.48×10^{-4}	22.1			
3	$+sc \rightleftharpoons -sc$	TLA	116		65	19.7[c]	19.3±0.6	−1.2±1.6	$C_6D_5CD_3$
			104		27				
		ST	65		1.16				
			57		0.58				
			48		0.27				
			39		0.11				
	$ap \longrightarrow \pm sc$	ST	105	6.5	1.63	21.9			
			94	6.5	0.66	22.0			
	$\pm sc \longrightarrow ap$	ST	118	6.5	0.42	23.8			
			105	6.5	0.18	23.6			
			94	6.5	0.05	23.8			
4	$+sc \rightleftharpoons -sc$	TLA	98		89	18.6[c]	19.3±0.5	2.1±1.3	$C_6D_5CD_3$
			93		61				
			89		44				
			80		22				
			71		10.5				
		ST	49		1.43				
			42		0.77				
	$ap \longrightarrow \pm sc$	TLA	98	13	5.5	20.7[c]	21.3±2.1	1.6±5.8	$C_6D_5CD_3$
			93	15	3.3	[22.2[c]	22.9±4.1	2.1±11.4][d]	
			89	15	2.4				
			80	16	1.2				
			71	16	0.5				

a) TLA: lineshape analysis; ST: saturation transfer; CK: classical kinetics. b) At the temperature indicated unless otherwise stated. c) At 350 K. d) Values for the $\pm sc \rightarrow ap$ process.

method, rate constants for the $\pm sc \rightarrow ap$ isomerization were obtained as given in Table 4.

Rate constants for the $\pm sc \rightarrow ap$ process as well as the $+sc \rightleftharpoons -sc$ process in **2** were also obtained by ^1H total lineshape analysis (TLA) at higher temperatures using bromobenzene-d_5 as the solvent (Fig. 2). Three doublets, one ascribed to the isochronous 8/13-protons of *ap*-**2** and two due to the anisochronous protons of $\pm sc$-**2**, were observed at the lowest field of δ=ca. 7.7 with an intensity ratio of ca. 2:1:1 at ambient temperature. On raising the temperature, two doublets due to $\pm sc$-**2** broadened, coalesced into a single doublet at ca. 70°C, and then resharpened while the doublet due to the *ap*-**2** remained intact. Above ca. 110°C these two doublets began to broaden. Total lineshape analysis using the DNMR3 program[18] gave rate constants for the $+sc \rightleftharpoons -sc$ interconversion at five temperatures in the range of 59—86°C and those for the $\pm sc \rightarrow ap$ conversion at 125 and 135°C (Table 4). The free energies of activation for the $\pm sc \rightarrow ap$ process obtained by TLA agree well with those by classical kinetics despite of the different solvents.

The interconversion among rotamers of **3** was slower than that in **2**. The 8- and 13-protons of $\pm sc$-**3** showed only broadened signals and those of *ap*-**3** gave a sharp doublet even at 116°C in toluene-d_8. Rate constants for the $+sc \rightleftharpoons -sc$ process could be determined by TLA at only two temperatures as shown in Table 4. Therefore the saturation transfer (ST) experiments were resorted to, which could afford rate constants of a slower process and thus those at lower temperatures.[19,20] Rate constants for the $+sc \rightleftharpoons -sc$ process at four temperatures in the range of 39—65°C were obtained by the ST method. Eyring parameters for the process were calculated using both the TLA and ST data. As for the even slower $ap \rightleftharpoons \pm sc$ process in **3**, ST experiments at 94—118°C gave rate constants as shown in Table 4. The rate constants for the $ap \rightarrow \pm sc$ process and those for the $\pm sc \rightarrow ap$ process were independently obtained at 94 and 105°C. The ratio of the two rate constants at a given temperature should give the equilibrium constant K at that temperature, but the agreement with the observed K value was only fair presumably because the smaller rate constants were somewhat unreliable.

In the case of **4**, the methoxyl proton signals were

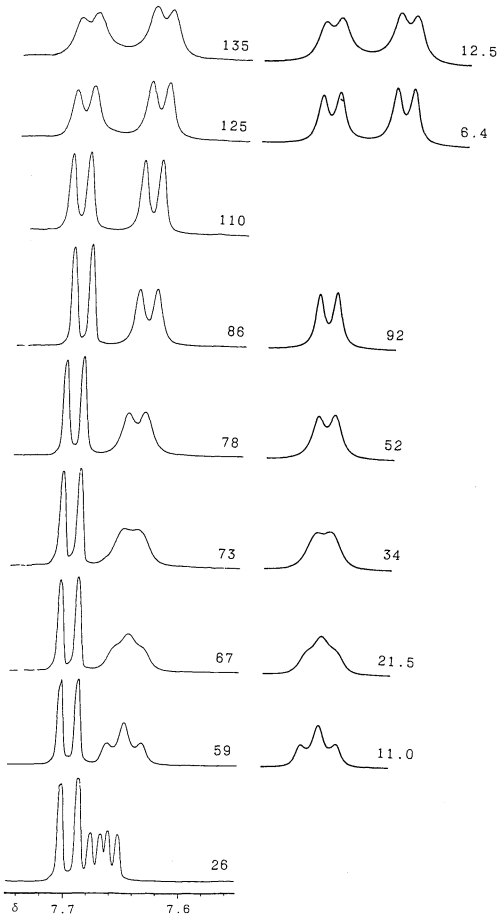

Fig. 2. Left: Spectra of the *peri*-protons of **2** in bromobenzene-d_5 at various temperatures (°C). Right: Calculated spectra with best-fit rate constants (s^{-1}).

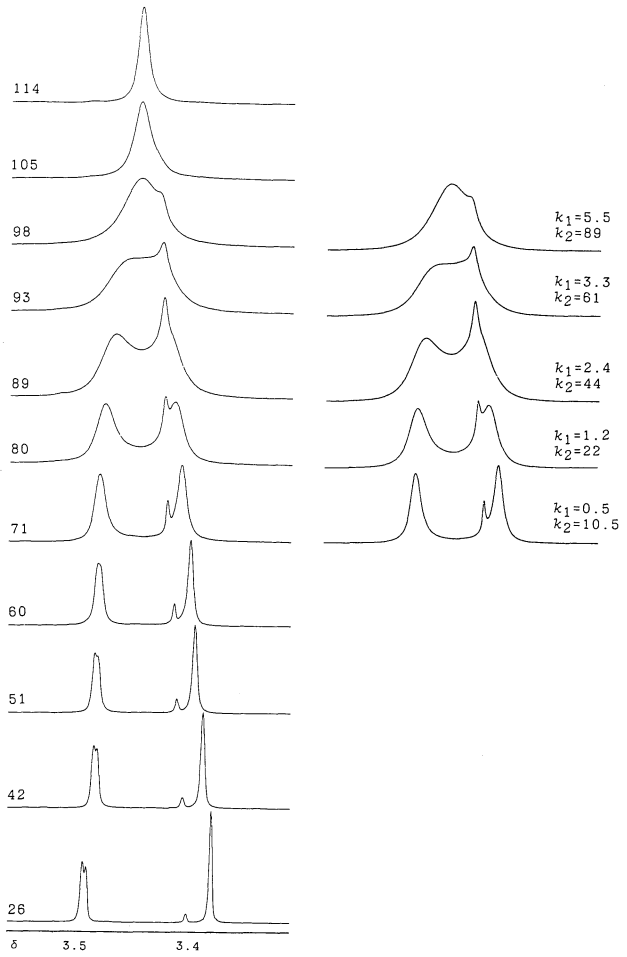

Fig. 3. Left: Spectra of the methoxyl protons of **4** in toluene-d_8 at various temperatures (°C). Right: Calculated spectra with best-fit rate constants (s^{-1}): k_1:$ap \rightarrow sc$, k_2:$+sc \rightleftharpoons -sc$.

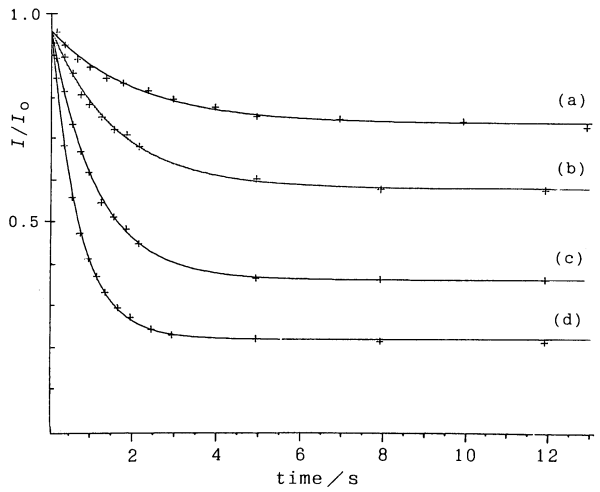

Fig. 4. Time dependence of the intensity of the 13-H signal of **3** upon irradiation of 8-H at (a) 39 °C, (b) 48 °C, (c) 57 °C, and (d) 65 °C. Experimental points are shown by + and the best-fit curves are given by solid lines.

suitable for the TLA study, affording rate constants for the $+sc \rightleftharpoons -sc$ and $ap \rightarrow \pm sc$ processes in the temperature range of 71—98 °C (Fig. 3). ST gave the $+sc \rightleftharpoons -sc$ rate constants at 42 and 48 °C.

As shown in Table 4, the $+sc \rightleftharpoons -sc$ process has a lower energy barrier than the $\pm sc \rightleftharpoons ap$ process in any compound. This may be reasonable because in the former process the methine hydrogen eclipses 1-F at the transition state while in the latter the oxygen moiety eclipses 1-F.

The $+sc \rightleftharpoons -sc$ barrier in terms of $\Delta G^{\ddagger}$ increases in the order of **2**<**4**<**3**, while the $ap \rightarrow \pm sc$ barrier increases in the order of **4**<**3**<**2**, although the increment is rather small. No simple correlation between the barrier heights and the geometries can be made.

Experimental

Melting points are not corrected. ^1H and ^{13}C NMR spectra were obtained on a Bruker AM-500 spectrometer operating at 500.1 and 125.8 MHz, respectively, in the pulse FT mode with internal tetramethylsilane as the chemical shift reference. ^1H chemical shifts were assigned on the basis of homonuclear double resonance and nuclear Overhauser effect (NOE) experiments. In variable temperature measurements, temperatures were calibrated using a methanol or ethylene glycol sample and are reliable to ±1 °C. In the ^{13}C data shown below, letters p, s, t, and q attached to the chemical shift values denote primary, secondary, tertiary, and quaternary, respectively. Signals are singlets under the ^1H noise-decoupled conditions unless otherwise stated. Chemical shift assignments, when indicated, were made by ^{13}C–^1H COSY experiments. In most compounds the signals due to carbons of the tetrafluorobenzeno moiety were not analyzed because of the complex splitting into very weak peaks.

9-(1,3-Dioxolan-2-yl)anthracene (5).[21] A solution of 10.3 g (50.0 mmol) of anthracene-9-carbaldehyde, 15 ml (ca. 0.27 mol) of 1,2-ethanediol, and 500 mg of *p*-toluenesulfonic acid in 200 ml of benzene are heated under reflux with a Dean-Stark apparatus for 20 h. The solution was chilled in an ice-water bath and quickly washed successively with cold aqueous sodium hydrogencarbonate and cold water and dried over magnesium sulfate. The filtered solution was concentrated to ca. 50 ml and 20 ml of hexane was added to cause crystallization of **5**. Yield 10.4 g (83%). ^1H NMR ($CDCl_3$) δ=4.22—4.31 (2H, m, 4′/5′-H), 4.46—4.55 (2H, m, 4′/5′-H), 7.095 (1H, s, 2′-H), 7.40—7.52 (4H, m, 2/3/6/7-H), 7.998 (2H, d, J=8.4 Hz, 4/5-H), 8.503 (1H, s, 10-H), 8.534 (2H, d, J=8.0 Hz, 1/8-H). The obtained material was used in the subsequent reaction without further purification.

9-(1,3-Dioxan-2-yl)anthracene (6). A similar procedure as above using 1,3-propanediol instead of 1,2-ethanediol gave **6** in 86% yield. Mp 153—154 °C. Found: C, 82.04; H, 6.04%. Calcd for $C_{18}H_{16}O_2$: C, 81.79; H, 6.10%. ^1H NMR ($CDCl_3$) δ=1.596 (1H, br d, J=11.1 Hz, 5′e-H), 2.581 (1H, m, 5′a-H), 4.185 (2H, m, 4′a/6′a-H), 4.447 (2H, m, 4′e/6′e-H), 6.907 (1H, s, 2′-H), 7.431 (2H, ddd, J=8.3, 6.5, and 1.0 Hz, 3/6-H), 7.514 (2H, ddd, J=9.0, 6.5, and 1.4 Hz, 2/7-H), 7.970 (2H, dd, J=8.4 and 1.2 Hz, 4/5-H), 8.450 (1H, s, 10-H), 8.783 (2H, dd, J=9.0 and 0.6 Hz, 1/8-H).

9-Dimethoxymethylanthracene (7).[22] A solution of 2.0 g (9.7 mmol) of anthracene-9-carbaldehyde in 20 ml of methanol containing a drop of concentrated hydrochloric acid was heated under reflux for 10 h. Cooling the solution resulted in crystallization of **7** (1.97 g, 80%). ^1H NMR ($CDCl_3$) δ=3.536 (6H, s, OCH_3), 6.554 (1H, s, $CH(OCH_3)_2$), 7.455 (2H, ddd, J=8.2, 7.5, and 1.0 Hz, 3/6-H), 7.503 (2H, ddd, J=8.9, 7.5, and 1.4 Hz, 2/7-H), 7.996 (2H, d, J=8.2 Hz, 4/5-H), 8.457 (1H, s, 10-H), 8.699 (2H, d, J=9.0 Hz, 1/8-H).

General Procedure for Addition of Tetrafluorobenzyne to the Anthracenes. To a chilled (−78 °C) solution of 1.0 ml (ca. 7.8 mmol) of chloropentafluorobenzene in 40 ml of diethyl ether was added dropwise 4.0 ml of a 10% (w/v) solution of butyllithium in hexane and the mixture was stirred for 2 h at −78 °C. To this solution was added 4.0 mmol of an appropriate anthracene acetal as powdery solids, and the mixture was allowed to warm up to room temperature, and then was heated under reflux for 15 h. The ^1H NMR spectrum of the crude reaction mixture revealed that the desired triptycene and the corresponding 1,4-adduct, i.e. 6-substituted 1,2,3,4-tetrafluoro-5,12-dihydro-5,12-ethenonaphthacene, were present in a ratio of ca. 1 : 1, together with a varying amount of the unreacted anthracene. The ethereal solution of the reaction mixture was stirred with 10 ml of 15% hydrochloric acid for 20 h at room temperature. The anthracene and the 1,4-adduct had been completely hydrolyzed to the respective formyl derivatives, while the triptycene remained as the acetal. Column chromatography of the mixture on alumina with hexane-dichloromethane as the eluent followed by recrystallization from hexane-dichloromethane gave the desired triptycene in a pure state.

9-(1,3-Dioxolan-2-yl)-1,2,3,4-tetrafluorotriptycene (2) was obtained in 19% yield. Recrystallization from dichloromethane–hexane gave a sample which consisted of two rotamers with a varying ratio [$\pm sc$]/[ap] of 1 to 3 but showed a constant mp of 228—230 °C. Found: C, 69.39; H, 3.43%. Calcd for $C_{23}H_{14}F_4O_2$: C, 69.35; H, 3.54%. An equilibrated solution of **2** in $CDCl_3$ consists of two rotamers, ap and $\pm sc$, in a ratio of 1 : 1.

Careful and slow recrystallization of **2** from dichloromethane–hexane gave selectively ±*sc*-**2** as crystals, mp 228—230°C. ^{1}H NMR ($CDCl_3$, 0°C) δ=4.05—4.52 (4H, ABCD-m, 4′/5′-H), 5.728 (1H, d, *J*=1.6 Hz, 10-H), 6.428 (1H, d, *J*=2.3 Hz, 2′-H), 7.04—7.13 (4H, m, 6/7/14/15-H), 7.39—7.45 (2H, m, 5/16-H), 7.68 (1H, m, 13-H), 7.73 (1H, m, 8-H); ^{13}C NMR ($CDCl_3$, 0°C, fluorinated carbons are omitted) δ=46.26t (10-C), 55.77q (br, 9-C), 64.90s (4′/5′-C, accidentally isochronous), 102.88t (d, *J*=4.7 Hz, 2′-C), 123.82t, 123.85t, 123.88t, 125.31t, 125.61t, 125.67t, 125.77t, 125.79t, 140.61q, 142.96q, 143.74q, 144.60q.

Careful and slow recrystallization of **2** from 2,2,4-trimethylpentane gave pure crystalline *ap*-**2**, mp 226—230°C. ^{1}H NMR ($CDCl_3$, 0°C) δ=4.30—4.36 (2H, *AA′*BB′, 4′/5′-H), 4.45—4.51 (2H, AA′*BB′*, 4′/5′-H), 5.760 (1H, d, *J*=1.4 Hz, 10-H), 6.277 (1H, d, *J*=4.9 Hz, 2′-H), 7.03—7.13 (4H, m, 6/7/14/15-H), 7.42 (2H, m, 5/16-H), 7.80 (2H, m, 8/13-H). ^{13}C NMR ($CDCl_3$, 0°C, fluorinated carbons are omitted) δ=46.08t (10-C), 57.43q (d, *J*=4.5 Hz, 9-C), 64.97s (d, *J*=3.2 Hz, 4′/5′-C), 102.11t (2′-C), 123.78t (5/16-C), 124.12t (8/13-C), 125.68t, 125.96t, 142.92q, 144.25q.

9-(1,3-Dioxan-2-yl)-1,2,3,4-tetrafluorotriptycene (3), mp 209—210°C, was obtained in 12% yield. Found: C, 69.86; H, 4.08%. Calcd for $C_{24}H_{16}F_4O_2$: C, 69.90; H, 3.91%. An equilibrated solution in $CDCl_3$ consists of two rotamers, ±*sc* and *ap*, in a ratio of 92:8. ^{1}H NMR ($CDCl_3$) ±*sc*-rotamer δ=1.622 (1H, br d, *J*=13.6 Hz, 5′e-H), 2.548 (1H, qt, *J*=12.9 and 5.1 Hz, 5′a-H), 4.187 (1H, td, *J*=13.2 and 2.5 Hz, 4′a-H or 6′a-H), 4.232 (1H, td, *J*=13.2 and 2.6 Hz, 4′a-H or 6′a-H), 4.421 (1H, br dd, *J*=11.5 and 5.1 Hz, 4′e-H or 6′e-H), 4.457 (1H, br dd, *J*=11.4 and 5.2 Hz, 4′e-H or 6′e-H), 5.701 (1H, d, *J*=1.3 Hz, 10-H), 6.206 (1H, d, *J*=2.3 Hz, 2′-H), 6.994 (1H, td, *J*=7.4 and 1.3 Hz, 6-H), 7.044 (1H, td, *J*=7.5 and 1.5 Hz, 7-H), 7.055 (1H, td, *J*=7.4 and 1.4 Hz, 15-H), 7.105 (1H, td, *J*=7.6 and 1.5 Hz, 14-H), 7.350 (1H, dd, *J*=7.3 and 1.3 Hz, 5-H), 7.399 (1H, dd, *J*=7.2 and 1.3 Hz, 16-H), 7.465 (1H, dd, *J*=7.6 and 1.0 Hz, 8-H), 8.369 (1H, dd, *J*=7.7 and 1.1 Hz, 13-H); *ap*-rotamer: δ=1.548 (1H, d, *J*=14.0 Hz, 5′e-H), 5.720 (1H, d, *J*=1.2 Hz, 10-H), 6.049 (1H, d, *J*=5.2 Hz, 2′-H), 7.515 (2H, dd, *J*=7.0 and 1.8 Hz, 8/13-H). ^{13}C NMR ($CDCl_3$) ±*sc*-rotamer δ=25.79s (5′-C), 46.48t (br, 10-C), 57.92q (d, *J*=3.7 Hz, 9-C), 67.58s (4′ or 6′-C), 67.65s (4′ or 6′-C), 101.23t (d, *J*=3.8 Hz, 2′-C), 123.53t (16-C), 123.73t (5-C), 123.66t (8-C), 125.34t (14-C), 125.53t (6- or 15-C), 125.54t (6- or 15-C), 125.84t (7-C), 127.30q (dt, *J*=12.2 and 3.0 Hz, 4a- or 9a-C)), 127.71 t (13-C), 130.27 q (dt, *J*=18.3 and 3.4 Hz, 4a- or 9a-C), 137.85q (dddd, *J*=253.0, 17.7, 12.8, and 3.0 Hz, 2- or 3-C), 138.43q (dddd, *J*=249.0, 20.1, 11.6, and 3.3 Hz, 2- or 3-C), 140.87q, 142.11q (ddt, *J*=243.2, 11.3, and 2.7 Hz, 1- or 4-C), 142.92q, 143.38q (ddd, *J*=250.2, 12.8, and 3.1 Hz, 1- or 4-C), 143.43q, 145.20q; *ap*-rotamer (fluorinated carbons are not detected) δ=24.52s (5′-C), 46.24t (d, *J*=3.0 Hz, 10-C), 66.89 s (4′/6′-C), 99.60 t (d, *J*=1.2 Hz, 2′-C), 123.66t, 124.20t, 125.48t, 125.74t, 143.07q, 144.75q.

Dissolution of the crystalline **3** in $CDCl_3$ below 0°C and immediate measurement of ^{1}H NMR at ca. 0°C showed that the sample consisted solely of ±*sc*-**3**.

9-Dimethoxymethyl-1,2,3,4-tetrafluorotriptycene (4), mp 217—218°C, was obtained in 12% yield. Found: C, 68.97; H, 4.13%. Calcd for $C_{23}H_{16}F_4O_2$: C, 69.00; H, 4.03%. An equilibrated solution in $CDCl_3$ consists of two rotamers, ±*sc* and *ap*, in a ratio of 97:3. ^{1}H NMR ($CDCl_3$) ±*sc*-rotamer δ=3.985 (3H, d, *J*=1.6 Hz, *sc*-OCH_3), 4.083 (3H, s, *ap*-OCH_3), 5.687 (1H, d, *J*=1.4 Hz, 10-H), 5.977 (1H, d, *J*=2.7 Hz, C*H*$(OCH_3)_2$), 7.013 (1H, td, *J*=7.4 and 1.1 Hz, 6-H), 7.061 (1H, td, *J*=7.4 and 1.4 Hz, 15-H), 7.068 (1H, td, *J*=7.5 and 1.5 Hz, 7-H), 7.093 (1H, td, *J*=7.5 and 1.6 Hz, 14-H), 7.298 (1H, br d, *J*=7.1 Hz, 8-H), 7.363 (1H, dd, *J*=7.2 and 1.3 Hz, 5-H), 7.394 (1H, dd, *J*=6.9 and 1.4 Hz, 16-H), 8.191 (1H, dd, *J*=7.5 and 1.4 Hz, 13-H); *ap*-rotamer δ=4.046 (6H, s, OCH_3), 5.711 (1H, d, *J*=1.2 Hz, 10-H), 5.798 (1H, d, *J*=4.4 Hz, C*H*$(OCH_3)_2$). ^{13}C NMR ($CDCl_3$, fluorinated carbons are omitted) ±*sc*-rotamer δ=46.53t (10-C), 60.07p (d, *J*=5.7 Hz, *sc*-OCH_3), 60.30q (d, *J*=3.3 Hz, 9-C), 60.57p (*ap*-OCH_3), 107.94t (d, *J*=3.3 Hz, *C*H$(OCH_3)_2$), 123.17t (8-C), 123.52t (16-C), 123.64t (5-C), 125.30t (14-C), 125.48t (6-C), 125.51t (7-C), 125.90t (15-C), 128.05t (13-C), 141.19q, 143.20q, 143.92q, 145.46q.

Dissolution of the crystalline **4** in $CDCl_3$ below 0°C and immediate measurement of ^{1}H NMR at ca. 0°C showed that the sample consisted solely of ±*sc*-**4**.

Molecular Mechanics Calculations. Molecular mechanics calculations were performed on a HITAC M-680H computer system at the Computer Center of the University of Tokyo using the BIGSTRN3 program[17] with a modified version of the MM2 force filed. As the parameters involving a fluorine atom attached to a benzene ring were lacking in the orginal force field, appropriate parameters were added as described before.[23] As BIGSTRN3 did not explicitly afford the values of dipole moments, the MM2 program[24] was used to calculate them using the geometries optimized by BIGSTRN3.

Total Lineshape Analysis. Total lineshape analysis was performed on an NEC PC-9801VX personal computer equipped with a Graphtec MIPLOT II plotter using the DNMR3K program, a modified version of DNMR3,[18] converted for use on a personal computer by Professor H. Kihara of the Hyogo University of Teacher Education.

In the case of **2** and **3**, the *peri* (8 and 13) proton signals were analyzed assuming a three-spin two-site system with inclusion of the couplings to the *o*- and *m*-protons (See Fig. 2). The two processes, $\pm sc \rightleftharpoons ap$ and $+sc \rightleftharpoons -sc$, could be separately analyzed disregarding the other process. In the case of **4**, the methoxyl signal was analyzed as a two-spin three-site system taking both processes simultaneously into account.

Temperature dependence of chemical shift differences, transverse relaxation times (T_2), and rotamer populations when necessary were properly taken into account.

Saturation Transfer Experiments. In the analysis of the $+sc \rightleftharpoons -sc$ interconversion in **3** and **4** in toluene-d_8, the 13-proton signal (δ=8.55 in **3** and δ=8.26 in **4**) was saturated by irradiation of a high frequency field and the 8-proton signal (δ=7.47 in **3** and δ=7.10 in **4**) was observed. The change in the signal intensity was followed as a function of the duration of the irradiation over the range of 1 ms to 12 s. Typical examples are shown in Fig. 4. The data were fitted to the exponential function (Eq. 1), and the three parameters, A, B, and C, were determined using the nonlinear least-squares method.[20]

$$I(t)/I_0 = A + B\exp(-t/C), \quad (1)$$

where $A=\tau_1/T_1$, $B=\tau_1/\tau$, $C=\tau_1$, and $1/\tau_1=1/\tau+1/T_1$. The rate constant k is given by $1/\tau$.

At several representative points, the 13-proton signal was observed upon irradiation of the 8-proton signal, which gave the same rate constants as obtained by the reverse procedure within the experimental error.

In the case of the $ap \rightleftharpoons \pm sc$ process in **3**, the α-H signals were used. Irradiation of the $\pm sc$ signal at δ=6.06 and observation of the *ap*-signal at δ=5.82 gave the $ap \rightarrow \pm sc$ rate constants and vice versa.

The present study was supported by a Grant-in-Aid for Scientific Research on Priority Areas No. 03214107 from the Ministry of Education, Science and Culture.

References

1) M. Ōki, *Acc. Chem. Res.*, **23**, 351 (1990).
2) E. L. Eliel, "Stereochemistry of Carbon Compounds," McGraw-Hill, New York (1962), pp. 156—179.
3) M. Ōki, *Angew. Chem., Int. Ed. Engl.*, **15**, 87 (1976); *Top. Stereochem.*, **14**, 1 (1983).
4) L. H. Schwartz, C. Koukotas, and C. S. Yu, *J. Am. Chem. Soc.*, **99**, 7710 (1977); L. H. Schwartz, C. Koukotas, P. Kukkola, and C. S. Yu, *J. Org. Chem.*, **51**, 995 (1986).
5) C. Rüchardt and H.-D. Beckhaus, *Angew. Chem., Int. Ed. Engl.*, **24**, 529 (1985); M. A. Flamm-ter Meer, H.-D. Beckhaus, K. Peters, H.-G. von Schnering, H. Fritz, and C. Rüchardt, *Chem. Ber.*, **119**, 1492 (1986).
6) G. Yamamoto and M. Ōki, *J. Chem. Soc., Chem. Commun.*, **1974**, 713; *Bull. Chem. Soc. Jpn.*, **48**, 3686 (1975); G. Yamamoto, M. Suzuki, and M. Ōki, *Angew. Chem., Int. Ed. Engl.*, **20**, 607 (1981); *Bull. Chem. Soc. Jpn.*, **56**, 306 (1983); G. Yamamoto, M. Suzuki, and M. Ōki, *Chem. Lett.*, **1980**, 1523; *Bull. Chem. Soc. Jpn.*, **56**, 809 (1983).
7) S. Otsuka, T. Mitsuhashi, and M. Ōki, *Bull. Chem. Soc. Jpn.*, **52**, 3663 (1979); S. Otsuka, G. Yamamoto, T. Mitsuhashi, and M. Ōki, *ibid.*, **53**, 2095 (1980); G. Yamamoto, A. Tanaka, M. Suzuki, Y. Morita, and M. Ōki, *ibid.*, **57**, 891 (1984).
8) M. Ōki, Y. Tanaka, G. Yamamoto, and N. Nakamura, *Bulll. Chem. Soc. Jpn.*, **56**, 302 (1983).
9) T. Tanaka, K. Yonemoto, Y. Nakai, G. Yamamoto, and M. Ōki, *Bull. Chem. Soc. Jpn.*, **61**, 3239 (1988); M. Ōki, T. Tanuma, Y. Tanaka, and G. Yamamoto, *ibid.*, **61**, 4309 (1988).
10) G. Yamamoto and M. Ōki, *Angew. Chem., Int. Ed. Engl.*, **17**, 518 (1978); *Bull. Chem. Soc. Jpn.*, **54**, 473 (1981); *ibid.*, **57**, 2219 (1984).
11) a) G. Yamamoto, *Chem. Lett.*, **1990**, 1373; b) G. Yamamoto, *ibid.*, **1991**, 741; c) G. Yamamoto, T. Nemoto, and Y. Ohashi, *Bull. Chem. Soc. Jpn.*, **65**, 1957 (1992).
12) a) F. Suzuki, M. Ōki, and H. Nakanishi, *Bull. Chem. Soc. Jpn.*, **47**, 3114 (1974); b) G. Yamamoto and M. Ōki, *ibid.*, **56**, 2082 (1983).
13) M. Suzuki, G. Yamamoto, H. Kikuchi, and M. Ōki, *Bull. Chem. Soc. Jpn.*, **54**, 2383 (1981).
14) H. Kikuchi, S. Hatakeyama, G. Yamamoto, and M. Ōki, *Bull. Chem. Soc. Jpn.*, **54**, 3832 (1981).
15) a) Y. Tanaka, G. Yamamoto, and M. Ōki, *Bull. Chem. Soc. Jpn.*, **56**, 3023 (1983); b) G. Yamamoto, Y. Tanaka, and M. Ōki, *ibid.*, **56**, 3028 (1983).
16) A part of the results has been published: G. Yamamoto, *Chem. Lett.*, **1991**, 1161.
17) R. B. Nachbar, Jr. and K. Mislow, QCPE Program No. 559.
18) D. A. Kleier and G. Binsch, QCPE Program No. 165.
19) S. Forsén and R. A. Hoffman, *J. Chem. Phys.*, **39**, 2892 (1963).
20) J. Sandström, "Dynamic NMR Spectroscopy," Academic Press, London (1982), Chap. 4.
21) G. Rio and B. Sillion, *Compt. Rend.*, **244**, 625 (1957).
22) J. S. Meek and J. R. Dann, *J. Org. Chem.*, **21**, 968 (1956).
23) G. Yamamoto and M. Ōki, *Bull. Chem. Soc. Jpn.*, **63**, 3550 (1990).
24) N. L. Allinger and Y. H. Yuh, QCPE Program No. 395.